scientific reports

Check for updates

OPEN

Dike-induced aquifer models derived from high-resolution multi-spectral satellite imagery

Samkelo Radebe & Martin Clark✉

The Main Karoo Basin in South Africa is a typical example of an expanding arid region dependent on groundwater resources. Dolerite dikes in the region, analogous to dolerite dikes worldwide, are known to influence subsurface groundwater flow and spatially relate to high-yielding boreholes. Here, the effect of dolerite dikes on groundwater flow is remotely assessed using the Modified Soil Adjusted Vegetation Index derived from high-resolution multi-spectral satellite imagery. From imagery collected during the wet and dry seasons of 2018 and 2021, two aquifer models relating to 505 dikes were identified; (1) barrier-controlled aquifers are induced by ~ 56% of dikes, (2) fractured aquifers are induced by ~ 35% of dikes. Surficial areas overlying aquifers are also shown to sustain vegetation growth through dry seasons. This research demonstrates the efficacy of vegetation indices to rapidly characterise dike-related aquifer models and their seasonal sustainability, critical for effective groundwater exploration and management.

Freshwater scarcity is a critical issue worldwide affecting an estimated 663 million people, with the dominant majority residing in developing countries[1]. The diminished availability of freshwater resources is exacerbated by climate change, through processes like desertification[2,3]. The Strategic Development Goals of the United Nations aim to ensure availability and sustainable management of freshwater and sanitation for all and recognize the need to take urgent action to combat climate change and its impacts[4]. As challenges to freshwater access relating to climate change are occurring more frequently, and increasing in severity, nations must undertake effective strategies to ensure freshwater access for their peoples[5,6].

In South Africa, 71% of the surficial landmass is currently classified as semi-arid or arid[7], and regions classified as subhumid are rapidly shrinking[8]. The western portion of the Main Karoo Basin (MKB) in South Africa has experienced a 48% decline in annual rainfall between 2013 and 2020, with median annual runoff less than 60 mm[9]. As a result, the surficial flow of water in the MKB is spatially and temporally sporadic, as exemplified by its western portion, resulting in 90% of communities to rely on regional deliveries, and local springs and boreholes, for water[9].

The MKB is a sedimentary basin, expressed over a 630,000 km^2 area, where groundwater exploration and management has been undertaken through traditional hydrological and geophysical surveying[10]. Aquifers in this area are mainly comprised of sandstones, mudstones, shale, and siltstones which are all low in permeability[11] and considered to be "complex and unpredictable" in their geohydrological behaviour[10]. Due to their complexity, local surveying has been critical to generate actionable information to explore for, and manage, aquifers in this area, albeit at significant cost[10].

High-yielding boreholes in the MKB (i.e., yielding between 13 and 85 l/s), are often associated with secondary geological structures such as dolerite dikes, ring structures, sill margins, and folded and faulted geological formations[10]. These geological structures manifest as lineaments when they intersect the surface[9]. The successful utilization of lineaments in groundwater exploration has been demonstrated in semi-arid regions of Australia, India, and Iran, where increased populations of lineaments within 0.1 to 3 km^2 areas have correlated with higher degrees of secondary porosity and by extension, larger volumes of available groundwater[12–15].

Groundwater accumulation in proximity to one type of lineament, dolerite dikes, is relative to the dike's width and the degree to which the dike has been deformed[16,17]. Less fractured dolerite dikes with widths greater than 10 m have been shown to create barrier-controlled aquifers adjacent to but only on one side of the dike (Fig. 1A)[17–19]. Baking of the host rock through contact metamorphism with the dike during emplacement, as well as shrinking of dike material during cooling, increases permeability that has been shown to create fractured aquifers along the dike (Fig. 1B)[11,20]. Considering the importance of geological lineaments in groundwater exploration, their uses in remote sensing studies have not sufficiently considered lineament types and the potentially variable effects they have on groundwater (Fig. 1A, B)[12,13,21–25].

Department of Geology, University of the Free State, Bloemfontein 9300, South Africa. ✉email: clarkmd@ufs.ac.za

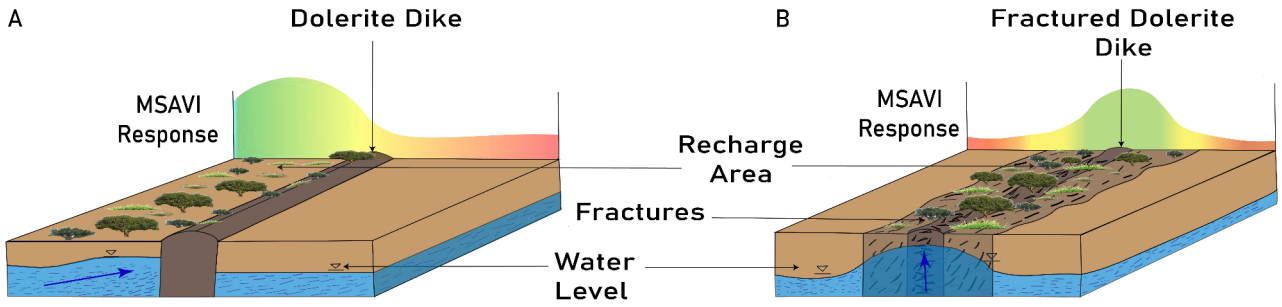

Fig. 1. Schematic models for a barrier-controlled aquifers (**A**) and fractured aquifer (**B**) illustrating the effect of a dolerite dike on groundwater levels. Note the surficial location of vegetation in **A** and **B** relative to the dolerite dike. Vegetation patterns are specifically displayed for arid and semi-arid regions.

The MKB exhibits a useful spatial correlation between surficial vegetation patterns and dolerite dike lineaments, where increased levels of vegetation correlate with proximity to dikes. This correlation has been observed in Ghana, where increased vegetation spatially correlates with high-yielding wells, suggesting increased vegetation is causational from increased availability of groundwater[26–28]. Both the high-yielding wells, and the increased vegetation occurred in proximity (<300 m) to dolerite dikes[26]. Recognizing areas with increased natural vegetation compared to their surrounding regions is rapidly accomplished using satellite-borne vegetation indices. Studies have shown that increased vegetation observed in dry seasons spatially correlate to areas of increased groundwater potential[29–31]. Therefore, to improve our ability to explore for groundwater in proximity to dolerite dikes, this study discriminates variable dike-induced impacts on groundwater potential in the MKB using the Modified Soil Adjusted Vegetation Index (MSAVI).

Results

Spatial affinity of elevated MSAVI (Modified Soil-Adjusted Vegetation Index) values to dolerite dikes in the Main Karoo Basin to characterise groundwater availability

The effect of woody vegetation on local biomass is observable in multi-spectral satellite imagery collected in dry seasons. Satellite-borne MSAVI shows biomass ranges for woody and diminutive vegetation are between 0.50 and 0.65, and 0.30 to 0.45, respectively. Provided an arid, or semi-arid area is non-riparian, vegetation growth is dependent on groundwater and therefore MSAVI values correlate to variability in the availability of groundwater. As dolerite dikes have widths defined in meters or tens of meters, MSAVI derived over large areas like the MKB result in stark spatial contrasts between areas with or without access to groundwater.

MSAVI was generated in the vicinity of 505 known dolerite dikes in 2018 and 2021 using PlanetScope multispectral satellite imagery. Whilst the total population of known dolerite dikes is 721, dikes located within agricultural, industrial, and human settlement areas, were excluded. Consequently, the analysis focused on 70% of known dolerite dikes. The 505 dikes had 37, 253, and 215 dikes located in subhumid, semi-arid zones, and arid climatic zones, respectively.

Across dike variability of MSAVI values

In 278 dikes (55%) observed in 2018, and 289 dikes (57%) observed in 2021, MSAVI values varied across dolerite dikes, e.g., Fig. 2 (Appendix A). The MSAVI values near the dike varied between the wet and dry seasons. During the wet season, the average MSAVI values were relatively high, ranging from 0.30 to 0.63, with little variability observed across the dike (Fig. 2A). Conversely, in the dry season, vegetation on the southwest side of the dike displayed greater MSAVI values compared to the northeast side where MSAVI values range in the dry season from 0.30 to 0.65 on the southwest side of the dike, versus 0.25 to 0.54 on the northeast side (Fig. 2B). This phenomenon of vegetation extended up to approximately 300 m from the dike. The MSAVI index values are investigated up to 400 m from the dike, and values of 0.25 and 0.65 are broadly representative of sparse grasses and moderate densities of woody vegetation, respectively (Fig. 2C). In the dry season, distances of 0 m to 150 m on the southwest side of the dike displayed the highest MSAVI values ranging between 0.60 and 0.65.

Along dike variability in MSAVI values

In 180 dikes (35%) observed in 2018 and 181 dikes (36%) in 2021, increased MSAVI values were found along dike traces, e.g., Fig. 3 (Appendix A). While seasonable variability in MSAVI values is apparent where MSAVI values for the wet season range higher than MSAVI values from the dry season, a narrow area of elevated MSAVI values was found within a ± 20-meter range from the dike trace (Fig. 3A, B, C). The index values in this narrow area range up to 0.42 in the dry season and up to 0.52 in the wet season. These values are + 0.12 and + 0.1 higher than the surrounding vegetation, which typically ranges up to 0.30 and 0.40 in the dry and wet season, respectively. Among the 181 dikes exhibiting this vegetation growth pattern in 2021, approximately 80 dikes are described by maximum MSAVI values below 0.50, and 101 dikes have maximum MSAVI values of 0.60, both observed in the dry season and indicative of woody vegetation.

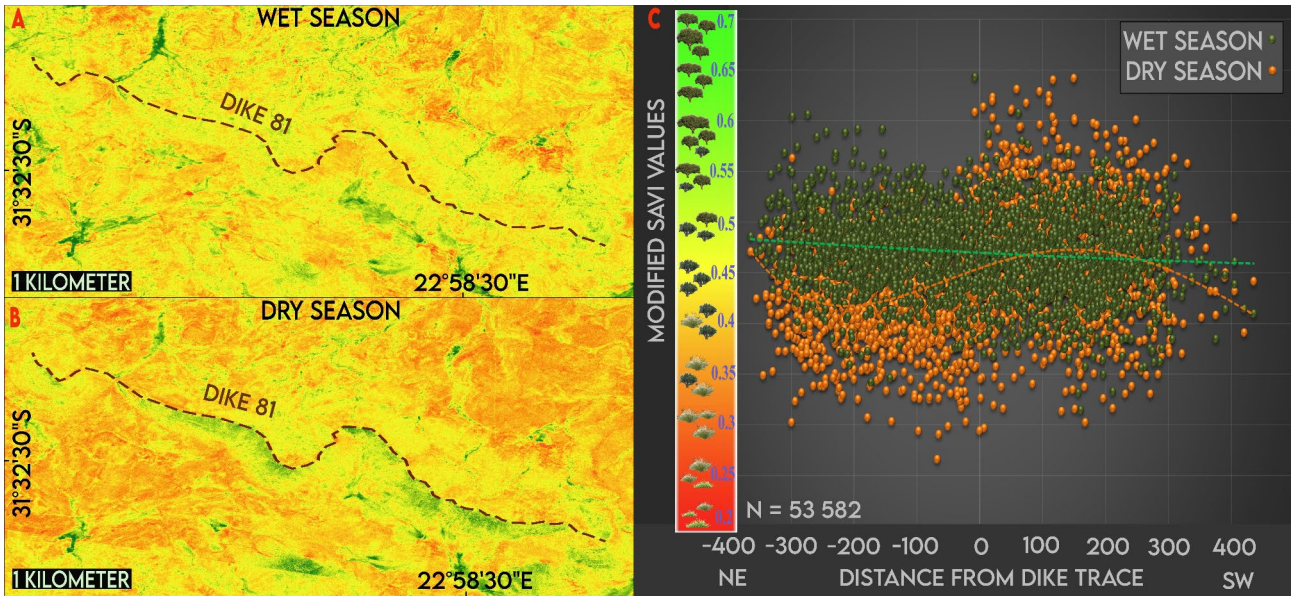

Fig. 2. Example of across dike variability in MSAVI value on Dike 81. (**A**) MSAVI values on 02 February 2021 during the wet season. (**B**) MSAVI values on 27 July 2021 during the dry season. A and B are oriented that North is towards the top of the page. (**C**) Graph of the MSAVI values across the dike trace to up to 400 m on either side. N indicates the number of MSAVI pixels. Trend lines were generated based on the best-fit function with the highest R^2 value illustrating variability between dry and wet season point clouds. MSAVI for A and B was generated in ENVI 5.5., and the maps were generated using ESRI ArcMap 10.8 and ESRI ArcGIS Pro 3.0.3.

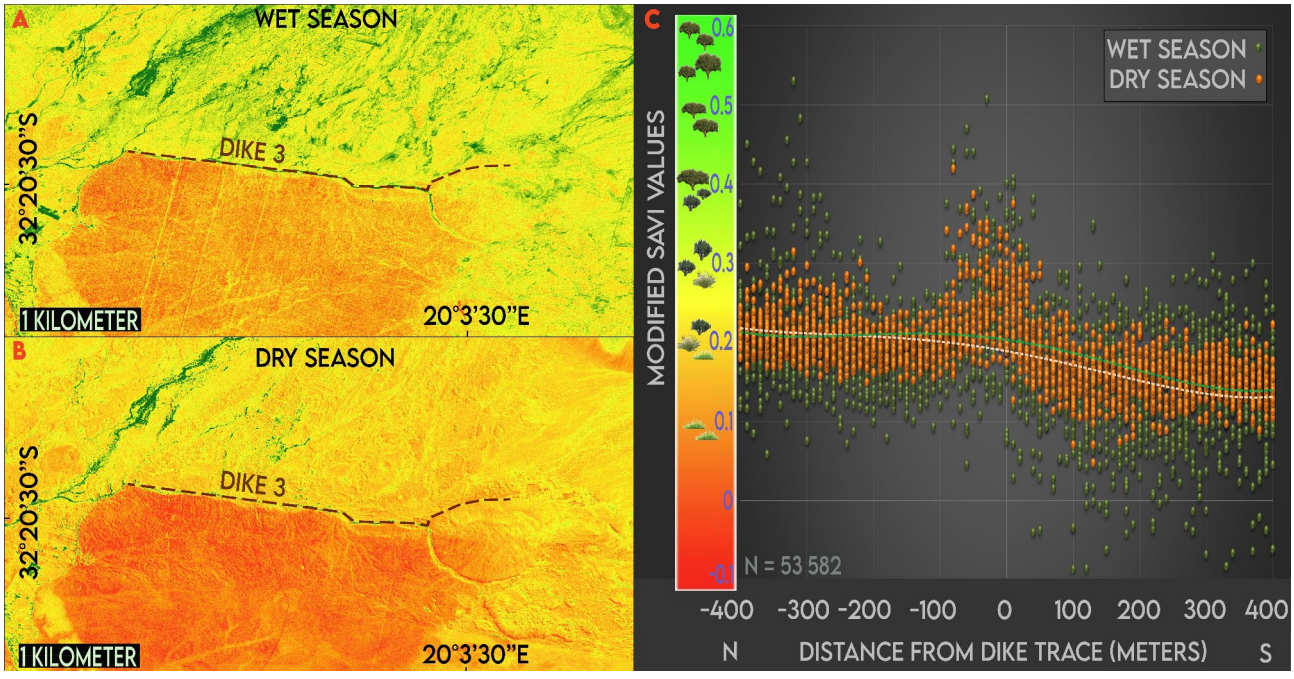

Fig. 3. Example of elevated MSAVI values along Dike 3. (**A**) MSAVI values on 29 December 2018 during of the wet season. (**B**) MSAVI values on 07 July 2018 during the dry season. A and B are oriented that North is towards the top of the page. (**C**) Graph of the MSAVI values across the dike trace to up to 400 m on either side. N indicates the number of MSAVI pixels. Trend lines were generated based on the best-fit function with the highest R2 value illustrating variability between dry and wet season point clouds. MSAVI for A and B was generated in ENVI 5.5., and the maps were generated using ESRI ArcMap 10.8 and ESRI ArcGIS Pro 3.0.3.

Discussion

The populations of MSAVI values from imagery collected in wet and dry seasons of 2018 and 2021 show the seasonal variability of vegetation as it relates to the availability of water (Figs. 2 and 3). During wet seasons, increased precipitation generally results in higher levels of vegetation, unless the area has insignificant precipitation regardless of the season, that then reduces during the following dry season. However, higher levels of vegetation persist through dry seasons when available groundwater is present. Here we show that dolerite dikes are a key and remotely observable mechanism for groundwater access and in the MKB. Proximity to dikes as historically applied is found to be insufficient to explain the spatial variability of the access or potential access to groundwater[20,32–34]. Based on the two observed vegetation patterns (e.g., Figs. 2 and 3), dolerite dikes in the MKB either induce barrier-controlled aquifers (Fig. 1A), or fractured aquifers (Fig. 1B).

Barrier-controlled aquifers in the MKB occur at ~ 56% of the dikes corroborating the only comprehensive regional study that addresses barrier-controlled aquifers as they relate to dolerite dikes (Fig. 2, Appendix A)[11]. Regionally significant borehole yields of 2 to 3 l/s were shown to have a spatial affinity to dolerite dikes[11]. However, the position of these boreholes relative to the dolerite dikes is unknown, and as shown here for dikes that induce barrier-controlled aquifers, the position of the borehole relative to the dike is an important consideration in whether a borehole will be high yielding or not. Therefore, published borehole yields may mischaracterise groundwater potential relating to barrier-controlled aquifers that are dike-induced when the borehole's position relative to dikes is not considered. Here, spatial variability in MSAVI provides a clear indication on which side of a dike may have induced a confined aquifer, as well as the locations along the dike where there are the highest levels of vegetation; a useful proxy to areas where the highest amounts of available groundwater are located. While this study shows confined aquifer models relate to > 50% of the dikes, a proximity-based approach to establishing boreholes relative to dikes would only have a ~ 50% chance to have maximized its effective yield.

Fractured aquifers are shown to occur at ~ 35% of the dikes, manifesting higher MSAVI values concentrated within a range of ± 20 m from the dikes (Fig. 3, Appendix A). This aligns with the potential to site high-yielding boreholes on, or directly adjacent to a dike[35]. Regionally significant fractured aquifer yields induced by dikes found that within ± 2 m from a dike yielding between 1.05 and 4.21 l/s, similar in yield to barrier-controlled aquifers[35]. The higher levels of vegetation that persist through dry seasons on and along dikes shows that there is sustained availability of groundwater, and therefore potentially the sustained yields from boreholes, even during periods when surface water is limited.

Complexities arise with the consideration of other parameters that relate to vegetation growth. Variable thicknesses and compositions of the regolith, extreme slopes where vegetation fails to take root, and vegetation species-specific water needs means care must be taken in correlating MSAVI to groundwater potential[36]. Some vegetation (e.g., Vachellia karroo) may access different depths of aquifers, meaning that their indication of groundwater availability may be regarding a deeper groundwater source rather than a shallower one[37,38]. However, with these complexities, each that should be studied and accounted for where they are observed to be significant, this approach shows the capacity to identify aquifer models, and areas of higher groundwater potential, rapidly and remotely.

A dike's effect on the type of aquifer is not necessarily exclusive (Fig. 3). Dike 3 demarcates a margin between a zone of generally higher MSAVI values to the north of the dike from a zone of generally lower MSAVI values to the south of the dike, consistent with a barrier-controlled aquifer (Fig. 3A, B). This variability of MSAVI values across the dike does not show a pronounced effect like the departure of MSAVI values on the dike. Therefore, the dike's effect to establish a fractured aquifer is dominant. The presence of variable effects is consistent with the known structural complexity of the MKB[10,16,39].

Based on our understanding of dike characteristics as they align to barrier-controlled aquifers (56%) and fractured aquifers (35%), this information may be used to further characterise the dolerite dikes, and regional vegetation variability as related to groundwater. For instance, in regions that are not geologically mapped, this approach may serve to identify geological dikes based on the effect they have on vegetation or enable further characterization of dikes such as thicknesses. Where fractured aquifers are identified, it can be suggested that those aquifers likely relate to dolerite dikes with widths of less than 10 m[16].

The variability of elevated MSAVI values in proximity to dolerite dikes is sometimes partially consistent with both aquifer models (Fig. 3, Appendix A). This is especially the case when the dike intersects a river as seen in Fig. 3 and suggests that additional inputs of water are present. Our approach avoided to study dikes where additional inputs of water were obvious (e.g., irrigation), meaning this study focused on 505 dikes instead of the total available population of 721, and explains why there is diminished capacity to visualise natural vegetation trends in proximity to dolerite dikes during wet seasons. The additional water from precipitation reduces our ability to remotely observe the complexity of subsurface flow networks (Appendix A).

This approach also cannot characterise aquifer models where groundwater flow networks may be minimal or non-existent within the accessible range of surface vegetation. This analysis could not characterise 9% of the dike population, that was primarily found in the most arid and subhumid regions of the MKB (Appendix A). A more sensitive vegetation index may be able to accentuate groundwater availability in these areas, however, if areas simply have no available groundwater, then no vegetation approach regardless how sensitive to vegetation growth is likely to work.

This study does not assess the impact of where a dike is located, it's orientation, or its thickness, which are important to further understand elevated MSAVI, and groundwater potential near dolerite dikes. Consequently, while the presence of vegetation near dikes may suggest the likely existence of near-surface aquifers, it does not provide any credible indication of the presence of deeper aquifers. For developing nations, the ability to drill deeper boreholes, or boreholes at all may not be available. Therefore, identifying where near-surface aquifers are, is critical for underdeveloped communities to consider where shallow wells may be best situated for their sustained access.

Whilst considering the drawbacks relating to this approach, its ability to rapidly characterise 505 dikes, characterize them as they pertain to two aquifer models, and to do so with 2–3 m of spatial accuracy, is novel and critical for effective regional groundwater management in the MKB and other areas undergoing aridification. This approach has provided a significantly better understanding of the geohydrological significance of dolerite dikes than undertaken in previous groundwater exploration studies that utilized a remote sensing approach[24,32–34,40].

This study utilized known dolerite dikes from the South African Council for Geoscience to thus ensure that dikes are accurately targeted to derive their effects on groundwater in the studied region. This approach can be adapted to regions where lineaments are not known. High-resolution imaging of an appropriate vegetation index to derive local groundwater behavior, can lead to subsurface structural mapping as it pertains to local geohydrological behavior. Areas where sharp vegetation contrasts can be identified, or lines of elevated vegetation can be delineated, can show the presence of confined and fractured aquifers, and indicate that dolerite dikes may be present, even if the dike is partially obscured by surficial overburden. Additionally, collecting imagery over protracted time frames can show how aquifers may evolve, vary in their ability to increase groundwater potential, and in cooperation with site specific borehole yields, be used to establish predictions of borehole yields based on climatic projections.

Conclusions

The presented study utilizing the MSAVI index to analyse groundwater-dependent vegetation in proximity to dolerite dikes offers a novel approach to characterise the local effect of dikes on groundwater. This study demonstrates that vegetation indices calculated from high-resolution imagery can reveal vegetation trends that indicate whether a dike has induced a confined or fractured aquifer, thereby contributing to informed decision-making in groundwater exploration, specifically borehole siting, and sustainable-yield assessments.

This study shows that dolerite dikes in the MKB have two effects, with ~ 56% of dikes inducing barrier-controlled aquifers, and ~ 36% of dikes inducing fractured aquifers. While this study has failed to characterise, dikes located in extreme arid areas, and in areas with anthropogenic activity, this study shows a consistent vegetation response to wet and dry season variability in 2018 and 2021, and that proximity to geological dikes as an exploration parameter to site boreholes, is insufficient in the MKB.

Increasingly rapid aridification induced by climate change makes it vital that we use various methodologies to ensure sustainable water access, especially in our most vulnerable regions. Our methodology describes a rapid and low-cost approach to study groundwater potential in proximity to one of Earth's most prolific geohydrologic feature: intrusive dolerite dikes. We advocate for the remote characterisation of the hydrological effects geological features can have, prior to engaging more invasive explorative or exploitative methods. We implore that public and private enterprises make use of remotely sensed data where it has sufficient spatial or spectral resolution and adopt proxy-based approaches to supplement their groundwater management in water-scarce regions where groundwater management is not-yet or only partially established.

Methods

Study area

The Main Karoo Basin (MKB) is located in the southeast escarpment of South Africa, between 28° and 34° S, and 10° and 32°E (Fig. 4). The MKB comprises of three structural domains expressed as dolerite dike distributions, these include the Western Karoo Domain, the Eastern Karoo Domain and the Transkei-Lesotho-Northern Karoo Domain[11]. In the Western Karoo Domain, sandstones and shales are intersected by dolerite sills and dikes to create fractured zones that enhance groundwater storage and flow[10,39]. The Eastern Karoo Domain is dominated by sandstones and mudstones which host fractured and confined aquifers where dolerite dikes intersect permeable sandstone layers. The Transkei-Lesotho-Northern Karoo Domain mainly comprise of sandstones, siltstones, and minor mudstones where dolerite dikes are known to play a key role in developing structurally controlled aquifers[10,39].

The MKB is classified as a retro arc foreland basin with a maximum preserved thickness of 6 km adjacent to the cape fold mountains and an average thickness of 3 km[41]. It is bounded by (1) a fold-thrust belt (Cape Fold Belt) lying along the southern margin of the basin, (2) the cratonic basement to the west, north and northeast, and (3) the Indian Ocean to the southeast.

The MKB is characterised by a climate that ranges from arid, semi-arid to sub-humid with annual precipitation of less than 200 mm per annum[11]. The MKB is characterized by areas that receive the bulk of precipitation in either the summer or winter months[42]. In regions with summer rainfall, the wet season typically occurs between November and March, with the peak rainfall from January to March[42]. The dry season generally extends from May to September, with the driest months being June to August[42]. Conversely, in areas receiving winter rainfall, the wet season spans from May to September, while the dry season usually lasts from November to March.

The surface elevation ranges between 800 m and 3650 m above sea level and is mainly expressed as flat-topped buttes and mesas "Koppies"[10]. Due to the low permeability of the lithologies that comprise the MKB, groundwater is generally classified as unreliable[10]. Nevertheless, secondary structures such as dolerite dikes, dolerite ring structures, dolerite sill margins (especially inclined sheets), thick alluvial deposits, and folded and faulted formations are hydrologically known for a higher potential for groundwater, especially where the host rocks are sandstones mudstones[16,35].

The vegetation of the MKB is typified by three prominent biomes: the Succulent Karoo biome, the Nama Karoo biome, and the Grassland biome. Given the region's scanty precipitation, vegetation primarily comprises of diminutive shrubs and grasses[37,38,43]. However, sporadic stands of woody vegetation comprising of Rhus undulata, Buddleja saligna, Euclea crisp avar. crispa, E. undulata var. undulata, Olea europaea, and Vachellia karroo are found, and the latter is the most widespread[37,38]. Thriving within riparian zones, woody vegetation

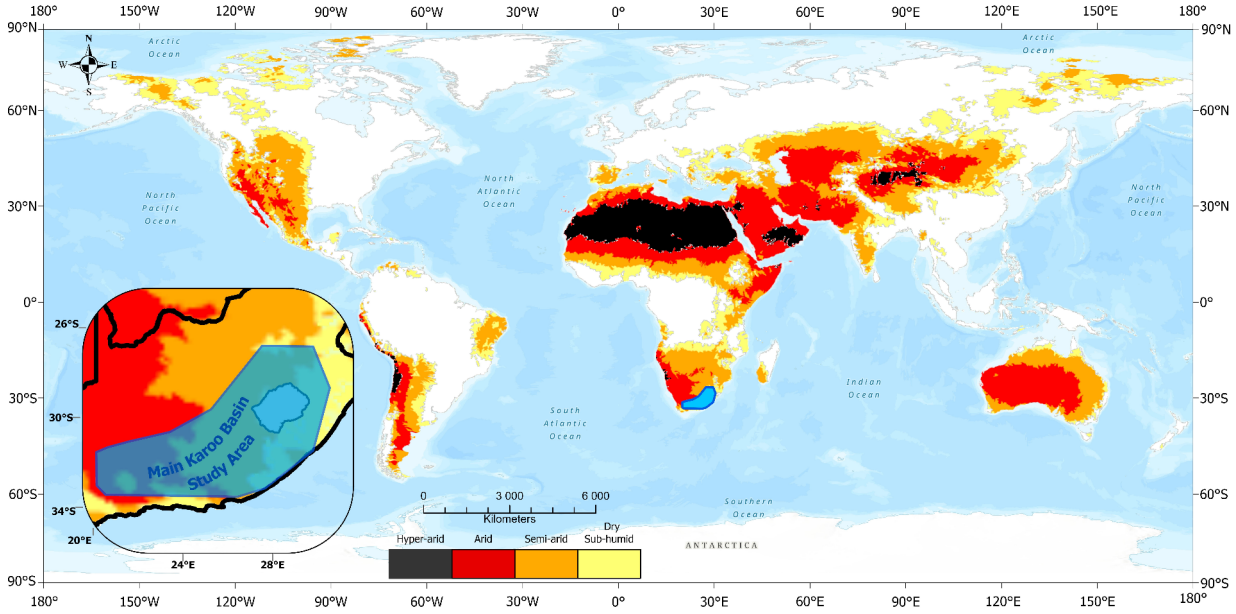

Fig. 4. Map of Earth showing the spatial distribution of the four most arid classes. The inset map delineates the study area within the central landmass of South Africa and the three climactic regions covered. Aridity data derived from[48]. ESRI World Topographic Map sourced from ArcGIS templates. The map was generated using ESRI ArcGIS Pro 3.0.3.

is indicative of sustainable access to water[43]. Vachellia karroo adapt their root systems to enable them to access deeper aquifers during periods of drought which also fosters the growth of smaller vegetation locally[44]. Therefore, Vachellia karroo has emerged as a reliable indicator of available groundwater during dry seasons[38,43].

Research design and materials

This study introduces a novel geographic information systems (GIS)-based workflow to analyse the Modified Soil Adjusted Vegetation Index MSAVI in the vicinity of dolerite dikes to characterise spatial groundwater availability (Fig. 5). This workflow uses Planet Labs PlanetScope Earth Imagery (https://www.planet.com/), with a spatial resolution of ~ 3 m and 4 spectral bands Blue (465–515 nm), Green (513–583 nm), red (650–680 nm) and Near-infrared (NIR: 845–885 nm), to generate the MSAVI[45]. We implemented this workflow using ENVI 5.5, ArcMap 10.8, ArcGIS Pro 3.0.3, Microsoft excel 2016, and the Spyder 5.4.5 Integrated Development Environment (IDE).

Data collection and pre-processing

PlanetScope satellite images were collected for the dry and wet seasons of 2018 and 2021. Most of the satellite images were geometrically and radiometrically corrected upon collection. However, some images had geometric errors that were corrected through co-registration in ENVI 5.5 to maintain a consistent geographic reference system of WGS 1984 UTM Zone 36 S. and any lasting radiometric errors such as haze, clouds and dark pixels were corrected using the haze removal, cloud masking and dark object removal tools on ENVI 5.5[46,47].

The 630,000 km^2 surface area covered by the MKB required creating a mosaic of the pre-processed satellite images (Fig. 4). However, due to variable image quality, smaller mosaics for specific areas were generated using histogram matching and edge feathering. Therefore, four mosaic images were generated for the North, South, West, and Eastern portions of the MKB generated for the wet and dry season of 2018 and 2021, respectively.

Modified SAVI Generation

The Modified SAVI index uses the near-infrared and red bands to enhance the reflectance of vegetation by reducing soil background noise, critical for arid regions with sparse vegetation such as the MKB (Fig. 4)[47]. The band ratio can be expressed as:

$$MSAVI = \frac{1}{2}[(2R_{NIR} + 1 - \sqrt{(2R_{NIR} + 1)^2 - 8(R_{NIR} - (R_{RED})} \quad (1)$$

where R_{NIR} is the near-infrared band, R_{RED} is the red band.

Characterising the effect of dolerite dikes on groundwater flow

To analyse groundwater flow along dolerite dikes, perpendicular transects were cast at 10 m intervals along the dikes on ArcGIS Pro 3.0.3. These were converted to points and used to extract both the Modified SAVI value at a specific location as well as the distance and direction that observation is to the position of the dike (Fig. 1A).

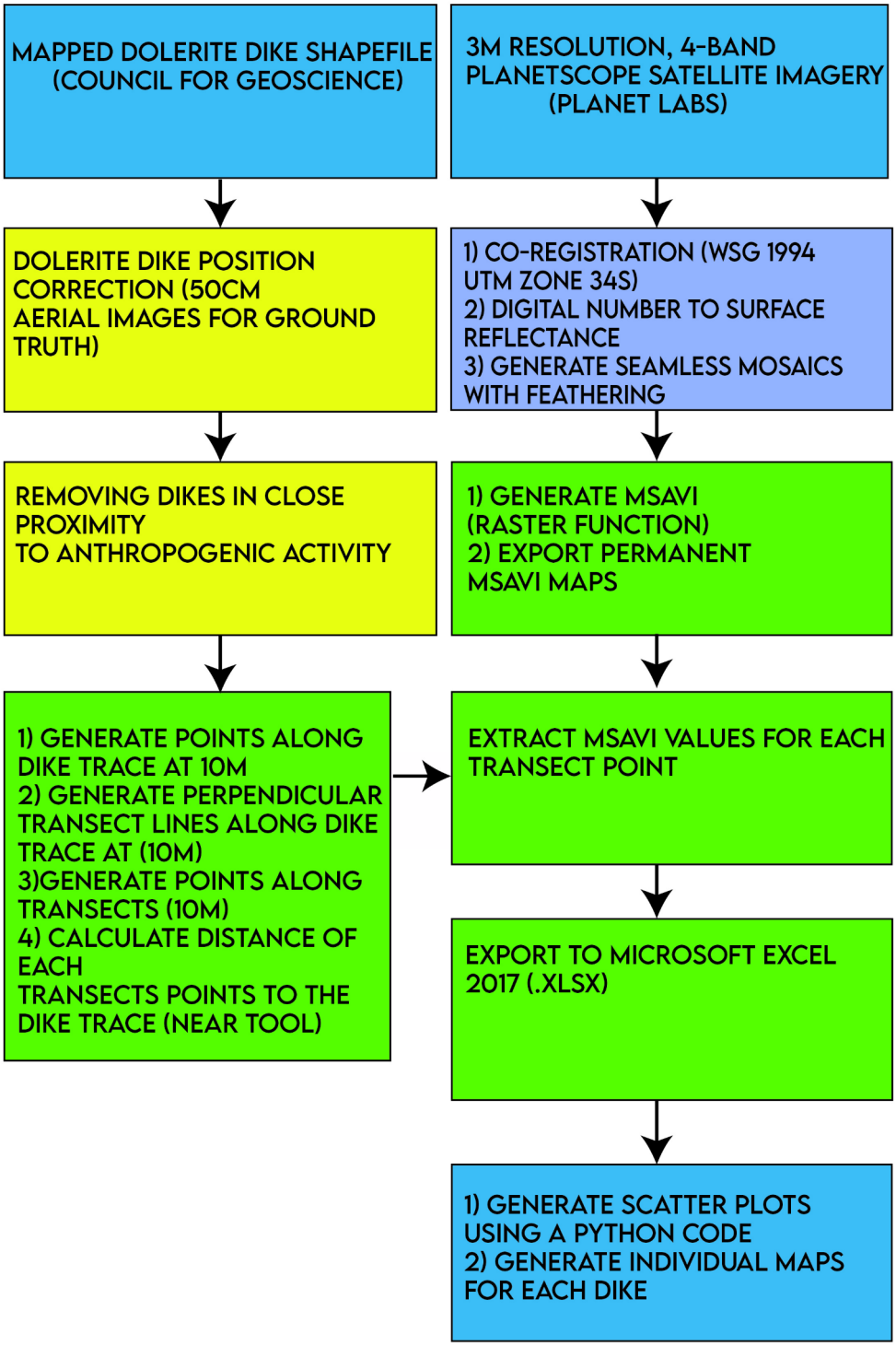

Fig. 5. Methodology flow chart for this study, yellow in the graph indicates work done on ArcMap 10.8, green indicates work done on ArcGIS Pro 3.0.3. All work done on ENVI 5.7 is illustrated with a purple colour.

Using excel the tables were pre-processed and prepared for python programming where point cloud graphs were generated using a python code on Spyder 5.4.5 (IDE) to analyse the change curve of Modified SAVI values with distance from a dolerite dike.

Data availability

MSAVI from planet lab imagery and graphical representations of MSAVI values for all studied dolerite dikes in the current study (Appendix A) are openly available in figshare at https://doi.org/10.6084/m9.figshare.25067690.

Received: 20 February 2024; Accepted: 4 October 2024
Published online: 10 October 2024

References

1. Viljoen, G. & van der Walt, K. South Africa's water crisis-an interdisciplinary approach. *Tydskrif vir Geesteswetenskappe*. **58**, 483–500 (2018).
2. Al-Ansari, N., Adamo, N. & Sissakian, V. Water shortages and its environmental consequences within Tigris and Euphrates Rivers. *J. Earth Sci. Geotech. Eng.* **9**, 27–56 (2019).
3. Bahta, Y. T. & Myeki, V. A. The impact of agricultural drought on smallholder livestock farmers: empirical evidence insights from Northern Cape, South Africa. *Agriculture*. **12**, 442 (2022).
4. Connor, R. *The United Nations World Water Development Report 2015: Water for a Sustainable World* vol. **1** (UNESCO publishing, 2015).
5. African Development Bank Group. *The Africa Water Vision for 2025: Equitable and Sustainable use of Water for Socioeconomic Development* (Economic Commission for Africa, Addis Ababa, 2000).
6. Cumming, T. L. et al. Achieving the national development agenda and the Sustainable Development Goals (SDGs) through investment in ecological infrastructure: a case study of South Africa. *Ecosyst. Serv.* **27**, 253–260 (2017).
7. Conradie, D. C. U. *South Africa's climatic zones: today, tomorrow*. (2012). https://researchspace.csir.co.za/dspace/bitstream/handle/10204/6064/Conradie2_2012.pdf?sequence=1&isAllowed=y
8. Jury, M. R. Spreading of the semi-arid climate across South Africa. *J. Water Clim. Change*. **12**, 3734–3749 (2021).
9. Hohne, D., Esterhuyse, C., Fourie, F., Gericke, H. & Esterhuyse, S. Enhancing groundwater recharge in the main Karoo, South Africa during periods of drought through managed aquifer recharge. *J. Afr. Earth Sc.* **176**, 104007 (2021).
10. Botha, J. F. et al. Karoo aquifers: their geology, geometry, and physical properties. *Water Research Commission Report No*. 487/1/98, 1–482 (1998).
11. Woodford, A. C. & Chevallier, L. Hydrogeology of the Main Karoo Basin: current knowledge and future research needs. *Water Res. Comm. Rep. no TT*. **179**, 482 (2002).
12. Epuh, E. E. et al. An integrated lineament extraction from satellite imagery and gravity anomaly maps for groundwater exploration in the Gongola Basin. *Remote Sens. Appl.* **20**, 100346 (2020).
13. Oyedele, A. A. Use of remote sensing and GIS techniques for groundwater exploration in the basement complex terrain of Ado-Ekiti, SW Nigeria. *Appl. Water Sci.* **9**, 1–13 (2019).
14. Das, S., Pardeshi, S. D., Kulkarni, P. P. & Doke, A. Extraction of lineaments from different azimuth angles using geospatial techniques: a case study of Pravara basin, Maharashtra, India. *Arab. J. Geosci.* **11**, 1–13 (2018).
15. Raj, N. J., Prabhakaran, A. & Muthukrishnan, A. Extraction and analysis of geological lineaments of Kolli hills, Tamil Nadu: a study using remote sensing and GIS. *Arab. J. Geosci.* **10**, 195 (2017).
16. Pacome, A. D. *Fracture characterisation of Karoo aquifers*. Doctoral dissertation, University of the Free State (2010).
17. Bromley, J., Mannström, B., Nisca, D. & Jamtlid, A. Airborne Geophysics: application to a ground-water study in Botswana. *Groundwater*. **32**, 79–90 (1994).
18. Babiker, M. & Gudmundsson, A. The effects of dykes and faults on groundwater flow in an arid land: the Red Sea Hills, Sudan. *J. Hydrol. (Amst)*. **297**, 256–273 (2004).
19. Comte, J., Wilson, C., Ofterdinger, U. & González-Quirós, A. Effect of volcanic dykes on coastal groundwater flow and saltwater intrusion: a field-scale multiphysics approach and parameter evaluation. *Water Resour. Res.* **53**, 2171–2198 (2017).
20. Van Wyk, W. L. *Ground-Water Studies in Northern Natal, Zululand and Surrounding Areas* (Department of Mines, 1963).
21. Hammouri, N., El-Naqa, A. & Barakat, M. An integrated approach to groundwater exploration using remote sensing and geographic information system. *J. Water Resour. Prot.* **4**, 1–8 (2012).
22. Bourjila, A. et al. Groundwater potential zones mapping by applying GIS, remote sensing and multi-criteria decision analysis in the Ghiss basin, northern Morocco. *Groundw. Sustain. Dev.* **15**, 100693 (2021).
23. Ejepu, J. S., Jimoh, M. O., Abdullahi, S. & Mba, M. A. Groundwater exploration using multi criteria decision analysis and analytic hierarchy process in Federal Capital Territory, Abuja, central Nigeria. *Int. J. Geosci.* **13**, 33–53 (2022).
24. Petrick, N. & Jubidi, M. F. Bin & Ahmad Abir, I. Groundwater potential Assessment of Penang Island, Malaysia, through integration of remote sensing and GIS with validation by 2D ERT. *Nat. Resour. Res.* **32**, 523–541 (2023).
25. Khadka, D. B. & Bhattarai, M. Delineation of ground water potential zoning using GIS and remote sensing by AHP of Sunsari district (Koshi Basin) Area of Nepal. *J. Eng. Res. Rep.* **24**, 42–61 (2023).
26. Sander, P., Chesley, M. M. & Minor, T. B. Groundwater assessment using remote sensing and GIS in a rural groundwater project in Ghana: lessons learned. *Hydrogeol. J.* **4**, 40–49 (1996).
27. Lubczynski, M. W. The hydrogeological role of trees in water-limited environments. *Hydrogeol. J.* **17**, 247 (2009).
28. Goldstein, G. et al. Water economy of neotropical savanna trees: six paradigms revisited. *Tree Physiol.* **28**, 395–404 (2008).
29. Song, G., Huang, J., Ning, B., Wang, J. & Zeng, L. Effects of groundwater level on vegetation in the arid area of western China. *China Geol.* **4**, 527–535 (2021).
30. Parizi, E., Hosseini, S. M., Ataie-Ashtiani, B. & Simmons, C. T. Normalized difference vegetation index as the dominant predicting factor of groundwater recharge in phreatic aquifers: case studies across Iran. *Sci. Rep.* **10**, 17473 (2020).
31. Zhang, G., Su, X. & Singh, V. P. Modelling groundwater-dependent vegetation index using Entropy theory. *Ecol. Modell.* **416**, 108916 (2020).
32. Solomon, S. & Quiel, F. Groundwater study using remote sensing and geographic information systems (GIS) in the central highlands of Eritrea. *Hydrogeol. J.* **14**, 1029–1041 (2006).
33. Ranganai, R. T. & Ebinger, C. J. Aeromagnetic and landsat TM structural interpretation for identifying regional groundwater exploration targets, south-central Zimbabwe Craton. *J. Appl. Geophy.* **65**, 73–83 (2008).
34. Akinluyi, F. O., Olorunfemi, M. O. & Bayowa, O. G. Investigation of the influence of lineaments, lineament intersections and geology on groundwater yield in the basement complex terrain of Ondo State, Southwestern Nigeria. *Appl. Water Sci.* **8**, 1–13 (2018).
35. Enslin, J. F. Geophysical methods of tracing and determining contacts of dolerite dykes in Karroo sediments in connection with the siting of boreholes for water. *S. Afr. J. Geol.* **53**, 193–204 (1950).
36. Zhu, X., Liu, H., He, W., Wu, L. & Liu, F. Regolith water storage patterns determine vegetation productivity in global karst regions. *Geoderma*. **430**, 116292 (2023).
37. Palmer, A. R. The vegetation of the karoo nature Reserve, Cape Province. I. A phytosociological reconnaissance. *South. Afr. J. Bot.* **55**, 215–230 (1989).

38. Palmer, E. & Pitman, N. Trees of Southern Africa: covering all known indigenous species in the Republic of South Africa, South-West Africa, Botswana, Lesotho & Swaziland. Volumes 1 & 2. *Trees of Southern Africa: covering all known indigenous species in the Republic of South Africa, South-West Africa, Botswana, Lesotho & Swaziland 1 & 2*. 1497 (1972).
39. Woodford, A. C. et al. *Hydrogeology of the main Karoo Basin: Current Knowledge and Research Needs* (Water Research Commission Report, 2001).
40. Magaia, L. A., Goto, T., Masoud, A. A. & Koike, K. Identifying groundwater potential in crystalline basement rocks using remote sensing and electromagnetic sounding techniques in central western Mozambique. *Nat. Resour. Res.* **27**, 275–298 (2018).
41. Catuneanu, O. et al. The Karoo basins of south-central Africa. *J. Afr. Earth Sc.* **43**, 211–253 (2005).
42. du Toit, J. C. O. & O'Connor, T. G. Changes in rainfall pattern in the eastern Karoo, South Africa, over the past 123 years. *Water SA*. **40**, 453–460 (2014).
43. Coates Palgrave, K. Trees of southern Africa. *Veld Flora*. **63**, 8 (1977).
44. Barnes, R. D., Filer, D. L. & Milton, S. J. *Acacia Karroo: Monograph and Annotated Bibliography* (Oxford Forestry Institute, Department of Plant Sciences, University of Oxford, 1996).
45. Frazier, A. E. & Hemingway, B. L. A technical review of planet smallsat data: practical considerations for processing and using planetscope imagery. *Remote Sens. (Basel)*. **13**, 3930 (2021).
46. Liu, W. & Yamazaki, F. Object-based shadow extraction and correction of high-resolution optical satellite images. *IEEE J. Sel. Top. Appl. Earth Obs Remote Sens.* **5**, 1296–1302 (2012).
47. Qi, J., Chehbouni, A., Huete, A. R., Kerr, Y. H. & Sorooshian, S. A modified soil adjusted vegetation index. *Remote Sens. Environ.* **48**, 119–126 (1994).
48. Peel, M. C., Finlayson, B. L. & McMahon, T. A. Updated world map of the Köppen-Geiger climate classification. *Hydrol. Earth Syst. Sci.* **11**, 1633–1644 (2007).

Acknowledgements

This study was supported by the Hans Merensky Legacy Foundation (UFS-AGR20-000248). Spatial geological data for dolerite dikes was accessed from the South African Council for Geoscience. Multispectral imagery was provided by Planet Labs. We thank Stephanus Riekert for his assistance with the python coding during the preparation of the figures, and the reviewers for their comments that helped to improve the accuracy of the text.

Author contributions

S.R., conceived and designed the methodology, processed the data, prepared the figures, and wrote the manuscript. M.C., conceived the study, edited the manuscript, and contributed to the discussion and significance of the findings.

Declarations

Competing interests

The authors declare no competing interests.

Additional information

Correspondence and requests for materials should be addressed to M.C.

Reprints and permissions information is available at www.nature.com/reprints.

Publisher's note Springer Nature remains neutral with regard to jurisdictional claims in published maps and institutional affiliations.